crystals

MDPI

Article

SiC_3 as a Charge-Regulated Material for CO_2 Capture

Haihui Zhang *, Huihui Xiong * and Wei Liu

School of Metallurgy Engineering, Jiangxi University of Science and Technology, Ganzhou 341000, China; pushful-liuwei@hotmail.com

* Correspondence: 9120160046@jxust.edu.cn (H.Z.); 9120120027@jxust.edu.cn (H.X.)

Abstract: The increasing CO_2 emission rate is deteriorating the atmospheric environment, leading to global warming and climate change. The potential of the SiC_3 nanosheet as a functioning material for the separation of CO_2 from the mixture of CO_2, H_2, N_2 and CH_4 by injecting negative charges is studied by DFT calculations in this paper. The results show that in the absence of injecting negative charges, CO_2 interacts weakly with the SiC_3 nanosheet. While the interaction between CO_2 and the SiC_3 nanosheet can be strengthened by the injection of negative charges, the absorption mechanism of CO_2 changes from physisorption to chemisorption when the injection of negative charges is switched on. $H_2/N_2/CH_4$ are all physiosorbed on the SiC_3 nanosheet with/without the injection of negative charges. The mechanism of CO_2 adsorption/desorption on the SiC_3 nanosheet could be tuned by switching on/off the injection of negative charges. Our results indicate that the SiC_3 nanosheet can be regarded as a charge-regulated material for the separation of CO_2 from the $CO_2/H_2/N_2/CH_4$ mixture.

Keywords: SiC_3 nanosheet; CO_2; adsorption; negative charges

Citation: Zhang, H.; Xiong, H.; Liu, W. SiC_3 as a Charge-Regulated Material for CO_2 Capture. *Crystals* **2021**, *11*, 543. https://doi.org/10.3390/cryst11050543

Academic Editors: Monica Distaso and Fabrizio Pirri

Received: 25 April 2021
Accepted: 11 May 2021
Published: 13 May 2021

1. Introduction

As the byproduct of human modernization activities, CO_2 is regarded as one of the significant causes of global warming and climate change. One of the main sources of carbon emissions comes from the use of coal as fuel or coke to reduce ores during extraction metallurgy. Taking iron and steel making for example, about 1.3~1.7 tons of CO_2 were exhausted per ton of steel produced in 2020, equating to about 8.0 percent of global carbon dioxide emissions. In the ferrous industry, most of the exhaust gases are reducing the atmosphere and contain the bulk of CO_2 that is emitted at temperatures higher than the ambient temperature. The typical blast furnace gas composition is N_2, CO, CO_2 and H_2 with the temperature of about 473~530 K, and the coke oven gas composition is N_2, CH_4, CO, CO_2 and H_2 with the temperature of about 1000 to 1300 K. CO_2 in the hot exhaust gas is expected to be collected and then reduced to CO that can facilitate the reduction reaction of CO_2 into synthetic fuels for a sustainable environment [1–4]. In the process of oxygen-converter steelmaking, CO_2 is a weaker oxidizing agent compared with O_2, and CO_2 can be reduced to CO by the C in the liquid hot metal [5,6]. Therefore, it is expected to develop an adsorbent material with the highly selective, controllable, and reversible of CO_2 capture that is high-temperature-resistant in the adsorption/desorption processes to fulfill the requirement of being in the metallurgy area.

Many 2D materials, due to their high surface area for CO_2 capture, have been synthesized or theoretically predicted [7], such as BN_2 [8], CN [9], C_2N [10], C_3N [11,12], PC_n [13], and Me–N–C (Me = Fe, Cu, Co, etc.) nanosheets [14,15], borophene nanosheet [16,17], covalent triazine frameworks [18], nanoporous grapheme [19], and penta-graphene [20]. Adding/removing the electrons to/from the adsorbent materials allows alteration of the affinity between the adsorbent materials and gases that is in favor of the CO_2 capture from the gas mixture [21]. Qin et al. [10] showed that the interaction between CO_2 and the C_2N nanosheet is enhanced by the negative charges or external electric field, and CO_2 molecules

are released from the C_2N nanosheet once the charge state/electric field is switched off. Li et al. [11] found that CO_2 molecules can be adsorbed and desorbed from the C_3N nanosheet by adjustment of the applying charge density. Tao et al. [22] found that the charged calcite is highly selective for separating CO_2 from the mixture of N_2, H_2 and CH_4, and the optimal charge density range for CO_2 capture and separation is 8.04~18.56 $\times$ 10^{13} e^-/cm^2. Other previous studies [8,10,11,13–15,17,18,21–25] also showed that the negative charges could be used as a switch in CO_2 capture and separation techniques by changing the affinity between CO_2 and the substrates, such as penta-BN_2, g-C_3N_4, nitrogen-doped porous carbons, etc.

Recently, works by Li and Shi et al. [26,27] showed that the silicon carbon monolayer possesses high thermal stabilities such that the Si_2C_3 and SiC_3 sheets can retain their planar geometries below 3500 K and manifest excellent properties of semiconductivity and elasticity for applications in electronics and optoelectronics. Chabi et al. [28] found that 2D silicon carbide (Si_xC_y) is a universal material, and exhibits the same properties as graphene, silicon or silicon carbide, depending on the composition (i.e., Si_2C_3, SiC_3 and SiC_4). For extensive exploration of novel nanostructures as potential materials for CO_2 capture, a question raised in this study is whether SiC_3 nanosheets are also a promising material for CO_2 capture, and whether its capture/separation could be efficiently tuned by the charge/electric field.

Therefore, the adsorption behaviors of CO_2, H_2, N_2 and CH_4 on the SiC_3 nanosheets with and without applying the injecting negative charges were studied by Density Functional Theory (DFT) calculations. Firstly, the stability of SiC_3 nanosheet with different gas molecule (i.e., CO_2, H_2, N_2 and CH_4) adsorption was explored. Secondly, the effects of the injecting negative charges on the electronic structure, bonding features of adsorption systems and the mechanism of the CO_2 adsorption/desorption on the SiC_3 nanosheet were studied. Finally, the possibility of CO_2 separation from the gas mixture with the assistance of negative charge, and the SiC_3 nanosheet as a promising CO_2 capture material were confirmed.

2. Calculation Method and Details

The calculations about the adsorption behavior of gas (i.e., CO_2, H_2, N_2 and CH_4) on the SiC_3 nanosheets were performed by using Density Functional Theory (DFT) methods, the implemented $Dmol^3$ module [29] with Generalized Gradient Approximation (GGA) and the Perdew–Burke–Ernzerhof (PBE) functional exchange correction functional. The details about the PBE functional have been well documented in the previous paper [30]. The effects of the core electrons were treated as a single effective potential by using the DFT semi-core pseudopotentials (USPP). Double numerical plus polarization (DNP) with a cutoff radius of 4.7 Å, and the DFT + D method with the weak van der Waals (vdW) correction were adopted in our calculations. Additionally, 4 $\times$ 4 $\times$ 1 k-points sampling of the SiC_3 nanosheet with 18 Si and 54 C atoms was adopted, and a 20 Å vacuum was set along the normal direction of the nanosheet for the elimination of the interactions between surface atoms. In geometric optimizations, the convergence tolerance was 1.0 $\times$ 10^{-5} Ha for the total energy, 0.002 Ha/Å for the maximum force, and 0.005 Å for the maximal displacement.

The adsorption energy (E_{ads}) of gas i on the SiC_3 nanosheet is described by the following equation [31,32]:

$$E_{ads} = E_{SiC_3,i} - E_{SiC_3} - E_i \quad (1)$$

where $E_{SiC_3,i}$ is the energy of the gas molecule i adsorbed on the SiC_3 nanosheet, E_{SiC_3} is the energy of the pure SiC_3 nanosheet, E_i is the energy of the isolated gas molecule i, and i indicates the gas molecule (i.e., CO_2, H_2, N_2 and CH_4). A lower value of E_{ads} corresponds to the stronger interaction between the SiC_3 nanosheet and gas molecule i, and thus, represents a more stable molecules adsorption structure.

The influence of the injecting negative charges on the stability of the SiC_3 nanosheet was studied, where the negative charges of numbers 0 to 5 e^- were injected into the SiC_3 nanosheet, equivalent to the negative charge densities of 0~2.06 $\times$ 10^{14} e^-/cm^2, which were applied on the SiC_3 nanosheet. For characterizing the adsorption of the gas molecule (i.e.,

CO_2, H_2, N_2 and CH_4) on the different, negatively charged SiC_3 nanosheet, the negative-charge density of the SiC_3 nanosheet (ρ) was investigated, and the negative charge density was defined as follows [10,17].

$$\rho = \frac{Q}{S} \tag{2}$$

where Q is the total negative charges injected into ($4 \times 4 \times 1$) the supercell of the SiC_3 nanosheet, and S is the corresponding surface area (2.43×10^{-14} cm^2).

To study the structural stability of a SiC_3 nanosheet under different negative-charge conditions, the phonon dispersion spectra and the cohesive energy are calculated. Generally, a larger cohesive energy corresponds to a more stable molecule-adsorption structure; also, no imaginary frequency in the phonon dispersion spectra indicates the stability of a material. The cohesive energy is defined as follows:

$$E_{coh} = \frac{n_c E_c + n_{Si} E_{Si} - E_{SiC_3}}{n_c + n_{Si}} \tag{3}$$

where E_c, E_{Si} and E_{SiC_3} are the energies of a single C atom, a single Si atom and the total energy of SiC_3 nanosheet, respectively. n_c and n_{Si} are the number of Si and C atoms in the SiC_3 nanosheet. Next, the effect of the injection of negative charges on the adsorption behavior of gas (i.e., CO_2, H_2, N_2 and CH_4) on the SiC_3 nanosheets was studied.

3. Results and Discussion

3.1. Electronic Properties and Stability of SiC_3 Nanosheet

The SiC_3 nanosheet is a graphene-like structure conformation with a P6/mmm space group. The calculated lattice constants of the primitive SiC_3 nanosheet are a = b = 5.584 Å. Figure 1a shows the deformation electron density of the $4 \times 4 \times 1$ fully relaxed supercell structure of the SiC_3 nanosheet. One can see that electrons are accumulated around the six-membered ring of carbon due to the larger, stronger electronegativity of carbon than that of silicon. The SiC_3 nanosheet has two different bonds, which are Si–C and C–C. The bonds lengths of Si–C and C–C are 1.796 and 1.428 Å, respectively, and the angle of C–C–C, C–C–Si and C–Si–C are all 120°. Those calculated results are in good agreement with the reported value [33]. For a pure SiC_3 nanosheet, the obtained Local Density of States (LDOS) of C and Si atoms are shown in Figure 1b. LDOS results show that the SiC_3 nanosheet exhibits a metallic characteristic due to several bands across the Fermi level that might be primarily contributed by the Si-p orbital [26]. The finding matches with the obtained results by Chabi et al. [28] that show that the SiC_3 nanosheet is a potential material for use as a semiconductor. Figure 1c shows the cohesive energy of the SiC_3 nanosheet under different charged conditions. The cohesive energy of a neutral SiC_3 nanosheet is 9.86 eV/atom, which is slightly larger than the reported value of neutral SiC_3 (7.84 eV/atom) [26]. The cohesive energy of the SiC_3 nanosheet is 9.86 eV/atom without the applied negative charge, and it decreases with increasing the applied negative charge, finally achieving a stable value (8.37 eV/atom) when the applied negative charge exceeds 3 e^{-1}. It is indicated that the SiC_3 nanosheet is a strongly bonded network and is a stable structure under the negative charge conditions. There is no imaginary frequency in the phonon dispersion spectra (Figure 1d). Therefore, all these results reflect the dynamic stability of the SiC_3 nanosheet under the condition of injecting negative charges. The SiC_3 nanosheet can withstand a rather high temperature under atmospheric pressure [26]. Therefore, the SiC_3 nanosheet is a stable material for CO_2 separation application after the injection of negative charges.

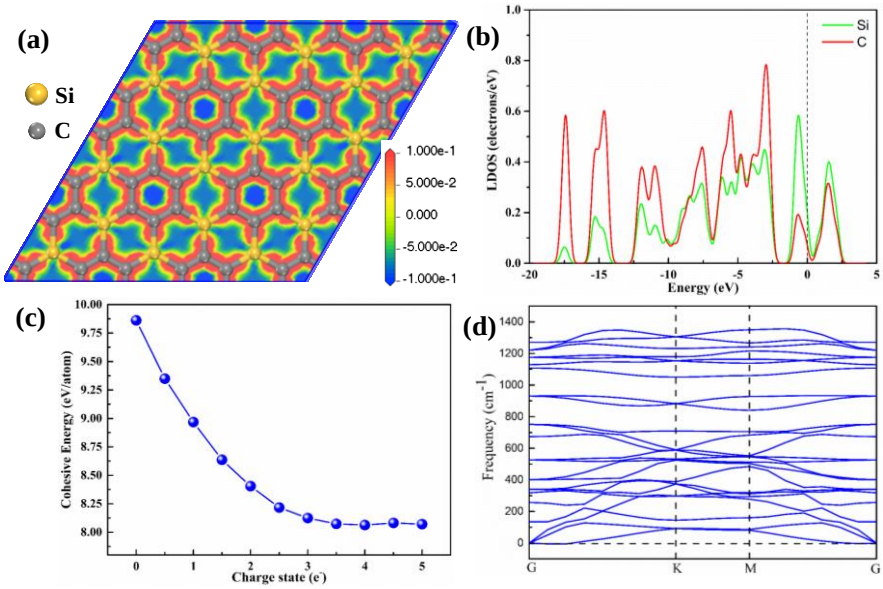

Figure 1. (**a**) Deformation electron density of SiC_3 nanosheet structure (4 × 4), (**b**) LDOS of the Si and C atoms of SiC_3 nanosheet with Fermi level set to 0 eV, (**c**) the cohesive energy of the SiC_3 nanosheet under different negative charge density conditions, and (**d**) the phonon dispersion spectra of SiC_3 nanosheet.

3.2. CO_2/H_2/N_2/CH_4 Adsorption on Uncharged SiC_3 Nanosheet

The gas adsorption behaviors of a neutral SiC_3 nanosheet is firstly investigated by analyzing the most stable relaxation configurations of the SiC_3 nanosheet with gas adsorption. Various initial adsorption sites are considered, including the top sites of C and Si atoms and bridge sites of C–C and C–Si bonds, as well as the center of hexagon holes. Stable relaxation configurations of the SiC_3 nanosheet with different gas molecule (i.e., CO_2, H_2, N_2 and CH_4) adsorptions are obtained and shown in Figure 2. For the most stable relaxation configurations, the CO_2, H_2, N_2 and CH_4 molecule distances from the SiC_3 nanosheet are 3.005, 2.6850, 3.235 and 3. 145 Å, respectively.

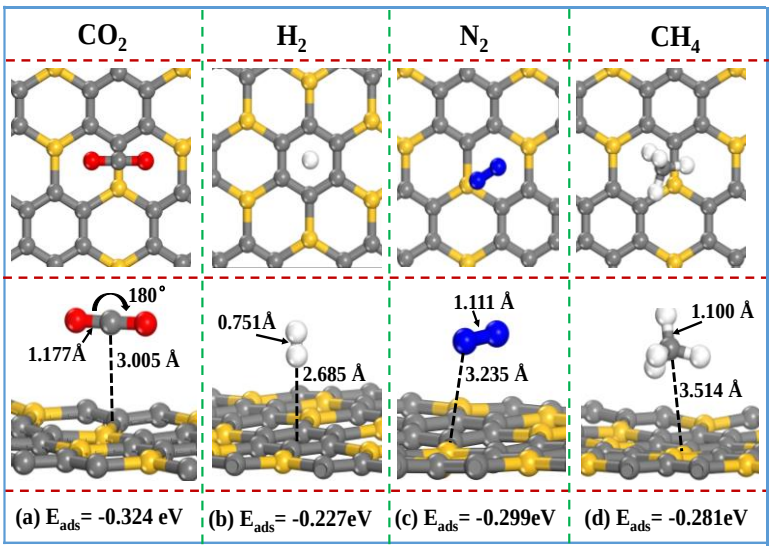

Figure 2. Top and side views of the stable adsorption configurations of different gas molecules adsorbed on the SiC_3 nanosheet without the injecting negative charges. (**a**) CO_2, (**b**) H_2, (**c**) N_2, and (**d**) CH_4 adsorbed on the SiC_3.

For the CO_2 adsorbed on the SiC_3 nanosheet, the O–C–O angle and the C–O bond length exhibit a minor change in comparison to the isolated carbon dioxide molecule, indicating that the absorption of CO_2 is classical physisorption. Similar results are observed for the H_2, N_2 and CH_4 molecule adsorbed on the SiC_3 nanosheet. Thus, it could be concluded that the gas molecules (i.e., CO_2, H_2, N_2 and CH_4) adsorbed on the SiC_3 nanosheet surface are caused by physisorption.

The adsorption energies (E_{ads}) of CO_2, H_2, N_2 and CH_4 adsorbed on the SiC_3 nanosheet are −0.324, −0.227, −0.299 and −0.281 eV, respectively. Among those four gases, the most stable relaxation configurations of gas molecules adsorbed on SiC_3 nanosheet are CO_2, followed by N_2, CH_4 and H_2, which indicates that the SiC_3 material is a potential material for use as a CO_2 adsorbent.

3.3. Adsorption of CO_2/H_2/N_2/CH_4 by Charged SiC_3 Nanosheet

With the injection of the negative charges with density of 1.23×10^{14} e^-/cm^2, the stable relaxation configurations of the SiC_3 nanosheet with different gas molecule (i.e., CO_2, H_2, N_2 and CH_4) adsorption are obtained and shown in Figure 3.

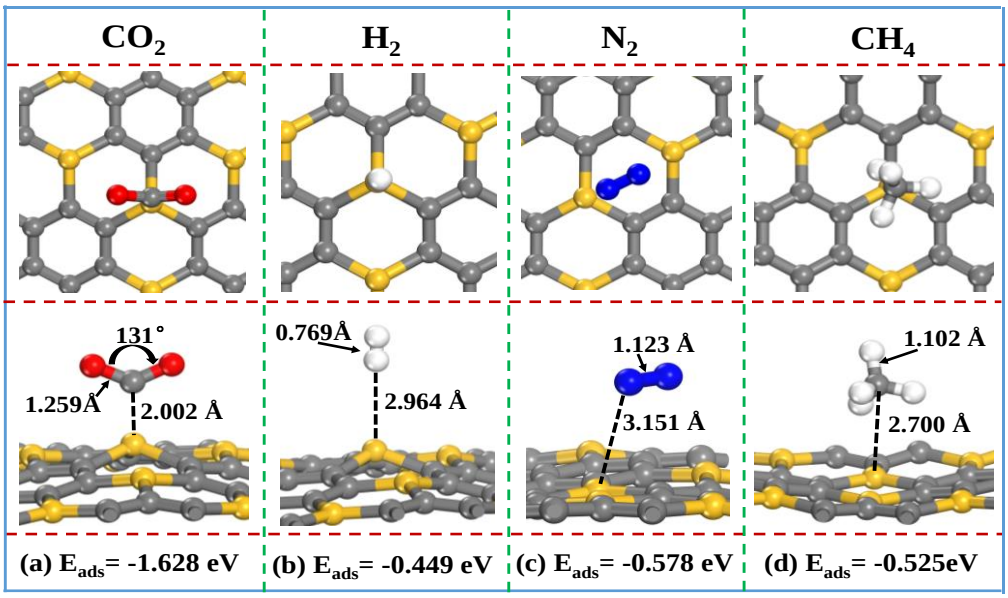

Figure 3. Top and side views of the stable adsorption configurations of different gas molecules adsorbed on SiC_3 nanosheet after the injection of the negative charges with density of 1.23×10^{14} e^-/cm^2. (**a**) CO_2, (**b**) H_2, (**c**) N_2, and (**d**) CH_4 adsorbed on the SiC_3.

After the injection of negative charges into the SiC_3 nanosheet with CO_2 absorption, the CO_2 molecule strongly interacts with the SiC_3 nanosheet with the adsorption energy E_{ads} of −1.628 eV; the adsorption energy is significantly smaller than that of the uncharged SiC_3 nanosheet (−0.324 eV). Furthermore, the O–C–O angle changes from 180° to 131°, the C–O bond length increases from 1.117 Å to 1.259 Å, and the distance between CO_2 and the SiC_3 nanosheet decreases from 3.005 Å to 2.002 Å. Obvious electron density distribution overlap is observed between CO_2 and the SiC_3 nanosheet (Figure 4e), indicating that the strong interaction between CO_2 and the SiC_3 nanosheet, and the absorption of the CO_2 molecule on the SiC_3 nanosheet is due to chemisorption.

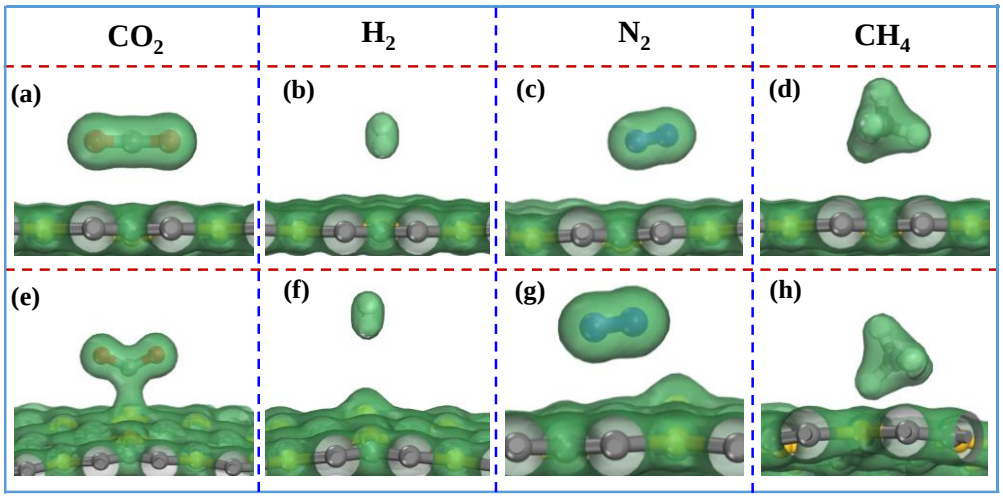

Figure 4. The electron density distribution of the most stable adsorption configurations of gas molecule (i.e., CO_2, H_2, N_2 and CH_4) adsorbed on the SiC_3 nanosheet. (**a**–**d**) Without the injecting negative charges, and (**e**–**h**) after the injection of negative charges with density of 1.23×10^{14} e^-/cm^2.

The optimized adsorption configurations of H_2, N_2 and CH_4 after the injection of negative charges are shown in Figure 3b–d. After the injection of negative charges into the SiC_3 nanosheet with H_2 absorption, for the H_2 molecule, the H–H bond length increases slightly from 0.751 to 0.769 Å, the distance between H_2 and the SiC_3 nanosheet increases slightly from 2.685 to 2.964 Å, and the adsorption energy E_{ads} decreases from −0.227 to −0.499 eV. For the N_2 molecule, the N–N bond length increases slightly from 1.111 to 1.123 Å, the distance between N_2 and the SiC_3 nanosheet decreases slightly from 3.235 to 3.151 Å, and the adsorption energy E_{ads} decreases from −0.299 to −0.578 eV. For the CH_4 molecule, the C–H bond length increases slightly from 1.100 to 1.102 Å, and the distance between CH_4 and the SiC_3 nanosheet decreases from 3.514 to 2.700 Å, and the adsorption energy E_{ads} decreases from −0.281 to −0.525 eV. Furthermore, no evident electron density distribution overlaps are observed between gas molecules (H_2, N_2 and CH_4) and the SiC_3 nanosheet after the injection of negative charges (Figure 4e). Thus, it is suggested that the adsorptions of H_2, N_2 and CH_4 on the SiC_3 nanosheet are due to physisorption with/without the injecting negative charges, which differs from the chemisorption of CO_2 on the SiC_3 nanosheet with the injection of negative charges.

Figure 4 shows no obvious electron density distribution overlaps observed between $CO_2/H_2/N_2/CH_4$ molecules and the SiC_3 nanosheet without the injecting negative charges. It indicates that $CO_2/H_2/N_2/CH_4$ interact weakly with the SiC_3 nanosheet without the injecting negative charges. However, after the injection of the negative charge with density of 1.23×10^{14} e^-/cm^2, obvious electron density distribution overlap between CO_2 and the SiC_3 nanosheet is observed. In other words, after the injection of the negative charges, the adsorptions of H_2, N_2 and CH_4 on the SiC_3 nanosheet are also due to physisorption with weak interactions between these molecules; when the adsorption mechanism of CO_2 on the SiC_3 nanosheet changes from physisorption to chemisorption, the interaction between CO_2 and the SiC_3 nanosheet gets stronger. These results suggest that CO_2 could be separated from the mixture of CO_2, H_2, N_2 and CH_4 that might be tuned by switching on/off the injection of negative charges.

3.4. Mechanism of CO_2 Adsorption/Desorption

The mechanism of CO_2 adsorption/desorption on the SiC_3 nanosheet are investigated by switching on/off the injection of negative charges. Figure 5 shows that the adsorption of CO_2 on the SiC_3 nanosheet is due to physisorption without the injection of negative charges. With the injection of negative charges with a density of 1.23×10^{14} e^-/cm^2, for the CO_2 molecule, the O–C–O angle changes from 180° to 131°, the C–O bond length increases from 1.117 Å to 1.259 Å, and the distance between CO_2 and the SiC_3 nanosheet

decreases from 3.005 Å to 2.002 Å. This result implies that the adsorption mechanism changes from physisorption to chemisorption; the analysis is consistent with the obtained results from Figure 4, and the process is exothermic with a reaction energy of −1.172 eV. After switching off the injection of negative charges, the adsorption mechanism of CO_2 changes from chemisorption to physisorption. The adsorbed CO_2 molecule is rebound to its physisorption state, and the distance between CO_2 and the SiC_3 nanosheet increases from 2.002 to 3.005 Å. This transition is also exothermic, 0.776 eV, without any energy barrier. In conclusion, the processes of CO_2 adsorption/desorption on the SiC_3 nanosheet is reversible, and CO_2 adsorption and separation would be tuned by switching on/off the injection of negative charges.

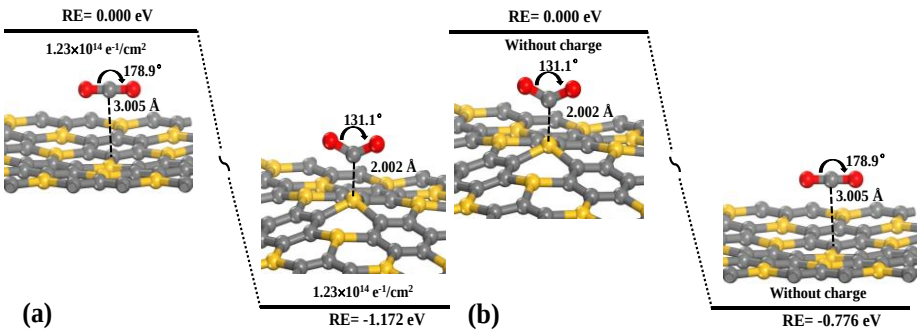

Figure 5. The process of (**a**) CO_2 adsorption on the SiC_3 nanosheet after injecting negative charges with density of 1.23×10^{14} e^-/cm^2 for the SiC_3 nanosheet with CO_2 adsorption, and (**b**) CO_2 desorption from the SiC_3 nanosheet after switching off the injection of negative charges.

3.5. Separation of CO_2 from H_2, N_2 and CH_4 on Negatively Charged SiC_3

The effect of the injection of negative charges on the interactions between gases and the SiC_3 nanosheet is shown in Figure 6. With the increase in negative charge density, the adsorption energy of CO_2 is smaller than those values of N_2, CH_4 and H_2. When the negative charge intensity exceeds 3.75×10^{13} e^-/cm^2, the adsorption energy of CO_2 adsorption decreases with the negative charge intensity observably, while the decrement of the adsorption energies for H_2, N_2 and CH_4 are relatively small. It is suggested that the CO_2–SiC_3 adsorption structure is more stable than the adsorption structures of N_2–SiC_3, CH_4–SiC_3, and H_2–SiC_3 under different charged conditions.

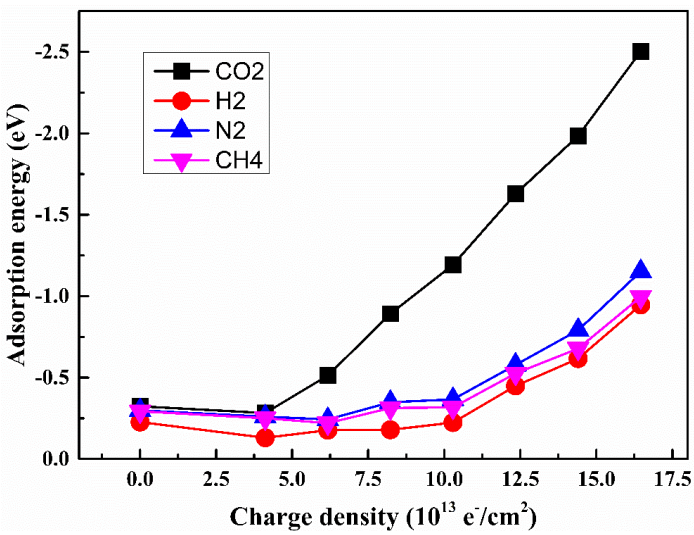

Figure 6. Effect of the injection of negative charges on the adsorption energy of the most stable configurations of SiC_3 nanosheet with CO_2, H_2, N_2 and CH_4 adsorption.

To further explore the CO_2 separation ability of the SiC_3 nanosheet by switching on/off the injection of negative charges, the co-adsorption behaviors of CO_2, H_2, N_2 and CH_4 on the SiC_3 nanosheet are investigated. As Figure 7 shows, after the injecting of the negative charges with a density of 1.23×10^{14} e^-/cm^2 into the SiC_3 nanosheet with gases co-absorption, the co-adsorption energy decreases from −0.255 to −0.976 eV. It implies that with the injection of negative charges, the SiC_3 nanosheet with gases (i.e., CO_2, H_2, N_2 and CH_4) co-absorption gets more stable in comparison with the one without the injection of negative charges.

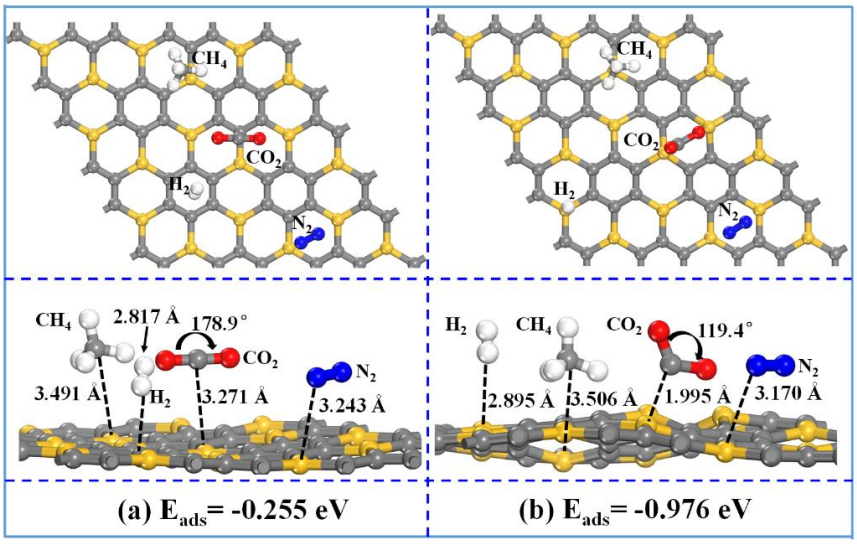

Figure 7. Top and side views of the optimized configurations of the SiC_3 nanosheet with gases molecules (i.e., CO_2, H_2, N_2 and CH_4) co-adsorption (**a**) without the injection of negative charges, and (**b**) with the injection of negative charges (1.23×10^{14} e^-/cm^2).

Switching on the injection of negative charges, the modules of H_2, N_2 and CH_4 move away from the SiC_3 nanosheet. The distance between the molecule and the SiC_3 nanosheet increases from 2.817 to 3.506 Å for H_2–SiC_3, from 3.243 to 3.170 Å for N_2–SiC_3, and from 3.491 to 3.506 Å for CH_4–SiC_3. No obvious electron density distribution overlaps are observed between $H_2/N_2/CH_4$ molecules and the SiC_3 nanosheet with/without the injection of negative charges (Figure 8). It indicates that the effect of the injection of negative charges on the adsorptions of $H_2/N_2/CH_4$ is not obvious, and $H_2/N_2/CH_4$ are all physiosorbed on the SiC_3 nanosheet with/without the injection of negative charges.

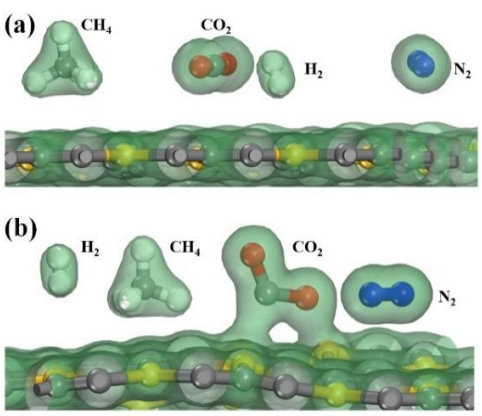

Figure 8. Top and side views of the charge density distribution of the SiC_3 nanosheet with gases molecules (i.e., CO_2, H_2, N_2 and CH_4) co-adsorption (**a**) without the injection of negative charges, and (**b**) with the injection of negative charges (1.23×10^{14} e^-/cm^2).

With the injection of negative charges into the SiC_3 nanosheet with gases co-absorption, the distance between the CO_2 molecule and the SiC_3 nanosheet gets shorter, decreasing from 3.271 to 1.995 Å, and the O–C–O angle of CO_2 changes from 178.9° to 119.4°. No obvious electron density distribution overlap is observed between the CO_2 molecule and the SiC_3 nanosheet without the injection of negative charges, while an obvious electron density distribution overlap is observed with the injection of negative charges (Figure 8), implying that the absorption mechanism of CO_2 changes from physisorption to chemisorption after the injection of negative charges, which is also consistent with the obtained results from Figure 5.

In summary, $H_2/N_2/CH_4$ all interact weakly with the SiC_3 nanosheet with/without the injection of negative charges. While the interaction between CO_2 and the SiC_3 nanosheet can be strengthened by the injection of negative charges, the absorption mechanism of CO_2 changes from physisorption to chemisorption after the injection of negative charges. Therefore, it could be concluded that the separation CO_2 from the mixture of CO_2, H_2, N_2 and CH_4 can be achieved by switching on/off the injection of negative charges. All of the above results demonstrate that the SiC_3 nanosheet is a promising material for the separation CO_2 from the $CO_2/H_2/N_2/CH_4$ mixture by using the injection of negative charges.

4. Conclusions

The potential of SiC_3 nanosheets as functional materials for the separation of CO_2 from the mixture of CO_2, H_2, N_2 and CH_4 by injecting negative charges is studied in this paper. The results show that the SiC_3 nanosheets are a promising material for the separation of CO_2 from the $CO_2/H_2/N_2/CH_4$ mixture. The main results are summarized as follows.

(1) In the absence of injecting negative charges, CO_2 interacts weakly with the SiC_3 nanosheet. While the interaction between CO_2 and the SiC_3 nanosheet can be strengthened by the injection of negative charges, the absorption mechanism of CO_2 changes from physisorption to chemisorption when the injection of negative charges is switched on.
(2) The effect of injecting negative charges on the SiC_3 nanosheet with $H_2/N_2/CH_4$ adsorption is not obvious, and $H_2/N_2/CH_4$ are all physiosorbed on the SiC_3 nanosheet with/without the injection of negative charges.
(3) The mechanism of CO_2 adsorption/desorption on the SiC_3 nanosheet could be tuned by switching on/off the injection of negative charges. The separation of CO_2 from the mixture of CO_2, H_2, N_2 and CH_4 can be achieved by switching on/off the injection of negative charges.

Author Contributions: Conceptualization, H.Z. and H.X.; methodology and software, H.X. and W.L.; validation and investigation, W.L. and H.X.; formal analysis, H.Z. and H.X.; writing—original draft preparation, W.L. and H.Z.; writing—review and editing, H.Z. and H.X.; supervision, H.X.; project administration, H.Z.; funding acquisition, H.Z. and H.X. All authors have read and agreed to the published version of the manuscript.

Funding: The authors gratefully acknowledge financial supports by the grants from the National Natural Science Foundation of China (No. 52074135), the Natural Science Foundation of Jiangxi Province, China (No. 20202BAB214016) and the Program of Qingjiang Excellent Young Talents, Jiangxi University of Science and Technology (No. JXUSTQJYX2020013).

Institutional Review Board Statement: Not applicable.

Informed Consent Statement: Not applicable.

Data Availability Statement: The data presented in this study are available within the article.

Conflicts of Interest: The authors declare no conflicts of interest.

References

1. Endrődi, B.; Samu, A.; Kecsenovity, E.; Halmágyi, T.; Sebők, D.; Janáky, C. Operando cathode activation with alkali metal cations for high current density operation of water-fed zero-gap carbon dioxide electrolysers. *Nat. Energy* **2021**, *6*, 439–448. [CrossRef]
2. Anwar, M.; Fayyaz, A.; Sohail, N.F.; Khokhar, M.; Baqar, M.; Khan, W.; Rasool, K.; Rehan, M.; Nizami, A. CO_2 capture and storage: A way forward for sustainable environment. *J. Environ. Manag.* **2018**, *226*, 131–144. [CrossRef] [PubMed]
3. Hu, Z.; Wang, Y.; Shah, B.; Zhao, D. CO_2 capture in metal–organic framework adsorbents: An engineering perspective. *Adv. Sustain. Syst.* **2019**, *3*, 1800080. [CrossRef]
4. Senocrate, A.; Battaglia, C. Electrochemical CO_2 reduction at room temperature: Status and perspectives. *J. Energy Storage* **2021**, *36*, 102373. [CrossRef]
5. Lv, M.; Zhu, R.; Bi, X.; Lin, T. Application research of carbon dioxide in BOF steelmaking process. *J. Univ. Sci. Technol. Beijing* **2011**, *33*, 126–130.
6. Dong, K.; Wang, X. CO_2 utilization in the ironmaking and steelmaking process. *Metals* **2019**, *9*, 273. [CrossRef]
7. Pardakhti, M.; Jafari, T.; Tobin, Z.; Dutta, B.; Moharreri, E.; Shemshaki, N.; Suib, S.; Srivastava, R. Trends in solid adsorbent materials development for CO_2 capture. *ACS Appl. Mater. Int.* **2019**, *11*, 34533–34559. [CrossRef] [PubMed]
8. Xiong, H.; Zhang, H.; Gan, L. CO_2 capture and separation on the penta-BN_2 monolayer with the assistance of charge/electric field. *J. Mater. Sci.* **2021**, *56*, 4341–4355. [CrossRef]
9. Talapaneni, S.; Singh, G.; Kim, I.; AlBahily, K.; Al-Muhtaseb, A.; Karakoti, A.; Tavakkoli, E.; Vinu, A. Nanostructured carbon nitrides for CO_2 capture and conversion. *Adv. Mater.* **2020**, *32*, 1904635. [CrossRef]
10. Qin, G.; Du, A.; Sun, Q. Charge-and Electric-Field-Controlled Switchable Carbon Dioxide Capture and Gas Separation on a C_2N Monolayer. *Energy Technol.* **2018**, *6*, 205–212. [CrossRef]
11. He, C.; Zhang, M.; Li, T.; Zhang, W. A novel C_6N_2 monolayer as a potential material for charge-controlled CO_2 capture. *J. Mater. Chem. C* **2020**, *8*, 6542–6551. [CrossRef]
12. Li, X.; Guo, T.; Zhu, L.; Ling, C.; Xue, Q.; Xing, W. Charge-modulated CO_2 capture of C_3N nanosheet: Insights from DFT calculations. *Chem. Eng. J.* **2018**, *338*, 92–98. [CrossRef]
13. Zhou, S.; Wang, M.; Wang, J.; Xin, H.; Liu, S.; Wang, Z.; Wei, S.; Lu, X. Carbon phosphides: Promising electric field controllable nanoporous materials for CO_2 capture and separation. *J. Mater. Chem. A* **2020**, *8*, 9970–9980. [CrossRef]
14. Li, X.; Zhu, L.; Chang, X.; He, D.; Xue, Q.; Xing, W. Me–N–C (Me = Fe, Cu, and Co) nanosheet as a promising charge-controlled CO_2 capture material. *J. Mater. Chem. A* **2018**, *6*, 12404–12410. [CrossRef]
15. He, C.; Wang, R.; Xiang, D.; Li, X.; Fu, L.; Jian, Z.; Huo, J.; Li, S. Charge-regulated CO_2 capture capacity of metal atom embedded graphyne: A first-principles study. *Appl. Surf. Sci.* **2020**, *509*, 145392. [CrossRef]
16. Wang, Z.; Lü, T.; Wang, H.; Feng, Y.; Zheng, J. Review of borophene and its potential applications. *Front. Phys.* **2019**, *14*, 1–20. [CrossRef]
17. Tan, X.; Tahini, H.; Smith, S. Borophene as a promising material for charge-modulated switchable CO_2 capture. *ACS Appl. Mater. Int.* **2017**, *9*, 19825–19830. [CrossRef]
18. Buyukcakir, O.; Je, S.H.; Talapaneni, S.N.; Kim, D.; Coskun, A. Charged covalent triazine frameworks for CO_2 capture and conversion. *ACS Appl. Mater. Int.* **2017**, *9*, 7209–7216. [CrossRef] [PubMed]
19. Sun, C.; Zhu, S.; Liu, M.; Shen, S.; Bai, B. Selective molecular sieving through a large graphene nanopore with surface charges. *J. Phys. Chem. Lett.* **2019**, *10*, 7188–7194. [CrossRef] [PubMed]
20. Wang, M.; Zhang, Z.; Gong, Y.; Zhou, S.; Wang, J.; Wang, Z.; Wei, S.; Guo, W.; Lu, X. Penta-graphene as a promising controllable CO_2 capture and separation material in an electric field. *Appl. Surf. Sci.* **2020**, *502*, 144067. [CrossRef]
21. Tan, X.; Kou, L.; Smith, S.C. Layered graphene-hexagonal BN nanocomposites: Experimentally feasible approach to charge-induced switchable CO_2 capture. *ChemSusChem* **2015**, *8*, 2987–2993. [CrossRef]
22. Tao, L.; Huang, J.; Dastan, D.; Wang, T.; Li, J.; Yin, X.; Wang, Q. CO_2 capture and separation on charge-modulated calcite. *Appl. Surf. Sci.* **2020**, *530*, 147265. [CrossRef]
23. Sathishkumar, N.; Wu, S.; Chen, H. Charge-regulated, electric-field and combined effect controlled switchable CO_2 capture and separation on penta-C_2N nanosheet: A computational study. *Chem. Eng. J.* **2021**, *407*, 127194. [CrossRef]
24. Tan, X.; Tahini, H.; Smith, S. Hexagonal boron nitride and graphene in-plane heterostructures: An experimentally feasible approach to charge-induced switchable CO_2 capture. *Chem. Phys.* **2016**, *478*, 139–144. [CrossRef]
25. Darvishnejad, M.; Reisi-Vanani, A. DFT-D3 calculations of the charge-modulated CO_2 capture of N/Sc-embedded graphyne: Compilation of some factors. *J. CO2 Util.* **2021**, *46*, 101469. [CrossRef]
26. Li, P.; Zhou, R.; Zeng, X. The search for the most stable structures of silicon–carbon monolayer compounds. *Nanoscale* **2014**, *6*, 11685–11691. [CrossRef] [PubMed]
27. Shi, Z.; Zhang, Z.; Kutana, A.; Yakobson, B.I. Predicting two-dimensional silicon carbide monolayers. *ACS Nano* **2015**, *9*, 9802–9809. [CrossRef] [PubMed]
28. Chabi, S.; Kadel, K. Two-Dimensional Silicon Carbide: Emerging Direct Band Gap Semiconductor. *Nanomaterials* **2020**, *10*, 2226. [CrossRef] [PubMed]
29. Delley, B. From molecules to solids with the $dmol_3$ approach. *J. Chem. Phys.* **2000**, *113*, 7756–7764. [CrossRef]
30. Qin, X.; Wu, Y.; Liu, Y.; Chi, B.; Li, X.; Wang, Y.; Zhao, X. Origins of dirac cone formation in ab_3 and a_3b (a, b = C, Si, and Ge) binary monolayers. *Sci. Rep-UK* **2017**, *7*, 1–13. [CrossRef]

31. Sharma, A.; Khan, M.; Husain, M. Adsorption of phosgene on Si-embedded MoS_2 sheet and electric field assisted desorption: Insights from DFT calculations. *J. Mater. Sci.* **2019**, *54*, 11497–11508. [CrossRef]
32. Jiao, Y.; Du, A.; Zhu, Z.; Rudolph, V.; Lu, G.; Smith, S. A density functional theory study on CO_2 capture and activation by graphene-like boron nitride with boron vacancy. *Catal. Today* **2011**, *175*, 271–275. [CrossRef]
33. Ding, Y.; Wang, Y. Geometric and electronic structures of two-dimensional SiC_3 compound. *J. Phys. Chem. C* **2014**, *118*, 4509–4515. [CrossRef]